energies

MDPI

Article

Optimal Integration of Hybrid Energy Systems: A Security-Constrained Network Topology Reconfiguration

Saman Nikkhah [1], Arman Alahyari [1,*], Adib Allahham [2] and Khaled Alawasa [3]

[1] School of Engineering, Newcastle University, Newcastle upon Tyne NE1 7RU, UK
[2] Faculty of Engineering and Environment, Northumbria University, Newcastle upon Tyne NE1 8ST, UK
[3] Department of Electrical Engineering, Mutah University, Mutah 61710, Jordan
* Correspondence: arman.alahyari@newcastle.ac.uk

Abstract: The integration of distributed energy resources, such as wind farms (WFs) and energy storage systems (ESSs), into distribution networks can lower the economic cost of power generation. However, it is essential to consider operational constraints, including loading margin, which ensures the security line contingency. This study aims to develop a comprehensive hourly distribution network reconfiguration (HDNR) model to minimize the economic cost for the power generation company. The model considers the optimal allocation of WFs and ESSs in terms of capacity and location, as well as the hourly status of the distribution network switches, based on security constraints. The proposed model is applied to an IEEE 33-bus distribution test system, and the capacities and locations of WFs and ESSs are determined. The impacts of security constraints on the optimal capacities and locations of WFs and ESSs, and the hourly configuration of the distribution network, are analyzed based on two case studies. In Case Study I, the model is solved with HDNR conditions, while Case Study II is solved without these restrictions, for comparison purposes. The results show that the optimal allocation of WFs and ESSs is affected by security constraints when HDNR is considered and highlight the crucial role of security constraints under contingency conditions, such as line outages. In the test system, three WFs and two ESSs are optimally allocated, with changes in capacity and location as the loading margin varies.

Keywords: wind farms; energy storage systems; optimal allocation; hourly distribution network reconfiguration; security; line contingency

Citation: Nikkhah, S.; Alahyari, A.; Allahham, A.; Alawasa, K. Optimal Integration of Hybrid Energy Systems: A Security-Constrained Network Topology Reconfiguration. *Energies* **2023**, *16*, 2780. https://doi.org/10.3390/en16062780

Academic Editor: Adrian Ilinca

Received: 19 February 2023
Revised: 11 March 2023
Accepted: 15 March 2023
Published: 16 March 2023

1. Introduction

As the world confronts the climate change issue, the primary objective is to shift towards a net-zero future by decreasing greenhouse gas emissions to a level that can be compensated by other measures [1,2]. The power industry is a key player in achieving this target since it generates a significant proportion of global emissions. The power sector will have to adopt cleaner and more sustainable energy sources, such as renewable energy, as well as enhance efficiency and minimize losses to achieve the net-zero objective [3]. To achieve this transition, integrating new technologies, such as distributed energy resources (DERs) and fast two-way communication, will be crucial to ensure grid reliability and stability [4,5].

The use of wind energy has seen tremendous growth in recent years due to its environmental and economic advantages. Projected wind total capacity in 2030, even with a steady growth, is more than 1200 GW worldwide, and this trend is expected to continue toward reaching ambitious environmental goals, such as net-zero emissions [6]. However, the delivery of wind power to consumers is challenged by operational and security issues, such as power losses and voltage instability, which are a result of the inherent intermittency of wind power generation. To overcome these issues, it is important to consider the security restrictions associated with wind power integration and investigate the coordination of energy storage systems [7].

Due to technical and economic limitations in expanding transmission systems, utilizing renewable DERs can play a crucial role in delivering power to customers, with lower active power losses and reduced environmental impact. The topology of distribution networks can also have a direct impact on the economic benefits of utilizing distributed generation. Although distribution networks typically have a mesh topology, they should be reconfigured to a radial configuration as much as possible to take advantage of the benefits of radial operation, such as short circuit current limiting and easy protection [8].

To achieve this, distribution network reconfiguration (DNR) is a solution in which the switches in the network are changed to reach a configuration that meets desired goals, while satisfying operational and security constraints, without isolating any network nodes. The optimization of DNR is necessary to ensure the proper operation of future distribution networks. It is also important to consider voltage stability constraints in the formulation of network reconfiguration studies. However, conventional DNR models may not be able to adapt to the increasing trends in network modernization, making an hourly DNR (HDNR) crucial for the proper operation of future distribution networks.

1.1. Literature Review

Recently, there has been a significant number of studies focused on the topic of distribution network reconfiguration, both with and without considering the impact of distributed generation. These studies have defined optimization objective functions based on both technical and economic aspects, as outlined in Table 1.

A review of these studies shows that formulating an objective function for DNR optimization based on economic factors is preferred, as it can encompass technical aspects and also reflect the economic benefits that can be realized from operating a distribution network with wind farms (WFs). In this subsection, we review several methodologies and techniques in the literature for solving the DNR problem. Ref. [6] shows the robustness of the proposed adaptive particle swarm optimization compared to the genetic algorithm for reconfiguration in the presence of DERs. The literature commonly uses power loss reduction as the objective in optimizing DNR in the presence of DERs, as seen in [8–11]. To address the issue of high-power losses and low reliability in the distribution network, ref. [12] proposed multi-objective reconfiguration models that simultaneously minimize power losses and improve system reliability. The proposed reliability indices include system average interruption frequency index, system average interruption duration index, and average energy not supplied. Amanulla et al. [13] focuses on a probabilistic reliability evaluation method for DNR due to the large computational time needed for reliability. The reconfiguration can also result in economic benefits for the network, as seen in [14], with the reduction of the annual cost after reconfiguration through minimization of power loss and reliability costs.

Load balancing is a technical objective in solving DNR, which is considered with power loss and reliability optimization in [15]. In that study, the non-dominated sorting genetic algorithm II is utilized to find solutions in a multi-objective modeling approach. Joen et al. [16] propose an optimal reconfiguration method for large distribution networks based on simulated annealing, which results in lower computational time compared to other studies. Ref. [17] employs graph theory based on radial DNR to improve computational performance, as well as the Pareto dominance rules of the reconfigured system. The enhanced gravitational search algorithm is used in [18] to improve processing time and the quality of reconfiguration results through special mutation strategy.

The integration of energy storage systems (EESs) is recently considered in DNR optimization. Nick et al. [19] propose a seasonal planning procedure to optimally allocate ESS capacity and location for DNR optimization. Ref. [20] focuses on coordinating power electronic devices, such as smart inverters, to decrease ESS investment costs through a planning schedule for ESSs in conjunction with distributed generators (DGs) and DNR. The application of ESSs to increase renewable DG unit penetration in the grid is studied in [21]. Studies [19–21] focus on long-term ESS planning with non-technical objectives, while [22]

considers voltage stability constraints in long-term DG planning to ensure power system security. Solving the problem from the DG owner's viewpoint can result in power losses and security criteria. This can result in exceeding normal values (i.e., normal operation of the system), since the main objective is to increase the penetration of wind energy into the grid for profit and other network characteristics.

While numerous studies have aimed to improve voltage profile through distribution network reconfiguration [5,6,11,19,23,24], none have considered developing an optimal reconfiguration model subject to voltage stability constraints. A sufficient voltage stability margin is crucial for distribution network security and should be considered in the DNR model. While voltage stability constraint models are widely used for power system optimization [4,22,25,26], they have not been applied to DNR studies. Table 2 summarizes the studies and their methodologies, available in the literature.

Table 1. Application of network reconfiguration in different optimization problems.

Objective	Target	Reference Number
Technical	Active power losses minimization	[6–18,23,24]
	Voltage profile improvement	[6,8,19,23,24]
	Reliability improvement	[12–14,17,18]
	Load balancing	[13,15]
	Switching costs	[9]
Economic	Operation costs	[6,14,18]
	Investment costs	[19–21]

Table 2. Summary of literature review of HNR studies.

Ref.	Objective Function		DER		Line Contingency	HDNR	Security	Optimal Allocation	
	Technical	Economic	DG	ESS				DG	ESS
[6]	✓								
[8]	✓		✓						
[9]	✓		✓						
[10]	✓		✓						
[11]	✓		✓						
[12]	✓	✓							
[13]	✓	✓							
[14]	✓	✓							
[15]	✓								
[16]	✓								
[17]	✓	✓							
[18]	✓	✓							
[19]		✓	✓	✓					✓
[20]		✓	✓	✓					✓
[21]		✓	✓	✓				✓	✓
[23]	✓								
[24]	✓								
This study		✓	✓	✓	✓	✓	✓	✓	✓

1.2. Contribution

The previous studies on DNR have examined various aspects, but there is a lack of research on security-constrained modeling for network reconfiguration involving the presence of wind farms and energy storage systems in order to minimize the economic cost for the generation company. Additionally, there have been no studies that focus on the hourly reconfiguration of the network with the optimal allocation of WFs and ESSs. Line contingency, which significantly affects the objective functions and decision variables, has not been taken into account in any DNR study. The objective of this study is to develop

a comprehensive HDNR model which minimizes the economic cost for the generation company (GenCo). The proposed model takes into account the optimal allocation of WFs and ESSs in terms of capacity and location, and specifies the hourly closed/opened switches of the distribution network based on security constraints.

The key features of this study include:

- Consideration of voltage stability as a security constraint for HDNR;
- Development of an HDNR model with a focus on minimizing the cost for the GenCo;
- Analysis of the impact of WFs and ESSs on the results of the proposed model;
- Joint allocation of WFs and ESSs with HDNR;
- Analysis of the sensitivity of HDNR to voltage stability constraints and vice versa;
- Analysis of the security of the reconfiguration model when line contingency occurs in the system.

The study is structured as follows: Section 2 presents the mathematical formulation of the model, while Section 3 provides the simulation parameters. Section 4 discusses the simulation results of the model applied to the IEEE 33-bus distribution test system. Finally, Section 5 concludes the study and proposes recommended actions.

2. Concept of the Network Security Index

The voltage stability margin, which is also known as the loading margin (LM), is an important criterion for measuring the security of the power system. This index is defined as the maximum power of generation units that can be increased to meet the load demand increase prior to violation of operational limits [4,26].

In order to guarantee the secure operation of the system, the network operator defines a specific level of LM. The assigned LM is defined as the difference between the initial operating point (IOP) and the maximum loadability point (MLP) in MW. The model defined in this study takes into account the power flow equations for IOP and MLP, simultaneously [22].

Figure 1 illustrates the concept of system security through the power–voltage (P-V) curve of an arbitrary load bus. In this figure, P_D^0 at point A is the load demand at IOP, while the voltage collapse point is point B. The loading parameter (λ_{des}) represents the desired LM which should be guaranteed during the operation of the system.

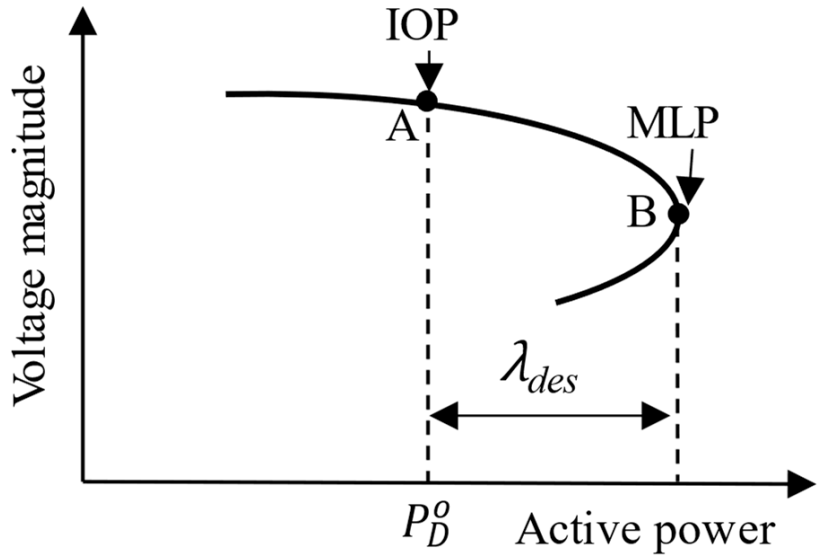

Figure 1. Concept of LM of arbitrary load bus [22].

3. Problem Formulation

The mathematical formulation of the proposed model, including the objective function, as well as operational and security constraints, are represented in this section. The description of symbols used in this section is given in the Nomenclature.

3.1. Objective Function

As stated in Table 1, the technical and economic aspects are the main objective functions of DNR formulation, where the latter could be inclusive of the former. The objective function defined in this study includes the cost of buying power from the main grid, the *WF* owners, and the GenCo, as stated below:

$$\min \ GC = \sum_{t=1}^{N_t} Cost_t^{WF} + Cost_t^{sub} \tag{1}$$

$$Cost_t^{WF} = \sum_{i=1}^{N_{WF}} S_{base} \times C_t^{pur} \times P_{i,t}^{WF} \tag{2}$$

$$Cost_t^{sub} = \sum_{i=1}^{N_s} S_{base} \times C_t^{pur} \times P_{i,t}^{G} \tag{3}$$

It is important to note that since the power stored in the *ESS* is from the main grid or the *WFs*, it is not included in the costs. The objective function of the proposed model is optimized based on several operational constraints, physical limits, and the radial configuration of the network. The power flow equations are considered simultaneously for both IOP and MLP.

3.1.1. Power Flow Constraints at IOP

The power flow equations at IOP are represented as follows:

$$P_{i,t}^{G} + P_{i,t}^{WF} + P_{i,t}^{CH} - P_{i,t}^{D} - P_{i,t}^{DICCH} = \sum_{j} (\delta_{ij,t}^{L} \times P_{ij,t}) \tag{4}$$

$$Q_{i,t}^{G} + Q_{i,t}^{WF} - Q_{i,t}^{D} = \sum_{j} (\delta_{ij,t}^{L} \times Q_{ij,t}) \tag{5}$$

$$P_{ij,t} = V_{i,t}^2 g_{ij} - V_{i,t} V_{j,t} (g_{ij} \cos\theta_{ij,t} + b_{ij} \sin\theta_{ij,t}) \tag{6}$$

$$Q_{ij,t} = -V_{i,t}^2 b_{ij} - V_{i,t} V_{j,t} (g_{ij} \sin\theta_{ij,t} - b_{ij} \cos\theta_{ij,t}) \tag{7}$$

$$\begin{cases} P_{sub}^{\min} \le P_{i,t}^{G} \le P_{sub}^{\max} & ; \forall i \in N_s \\ 0 & ; \text{otherwise} \end{cases} \tag{8}$$

$$\begin{cases} Q_{sub}^{\min} \le Q_{i,t}^{G} \le Q_{sub}^{\max} & ; \forall i \in N_s \\ 0 & ; \text{otherwise} \end{cases} \tag{9}$$

$$V_i^{\min} \le V_{i,t} \le V_i^{\max} \tag{10}$$

$$\delta_{ij,t}^{L} (I_{R_{ij,t}}^2 + I_{M_{ij,t}}^2) \le I_{MAX_{ij}}^2 \tag{11}$$

$$I_{R_{ij,t}} = g_{ij}(V_{i,t}\cos\theta_{i,t} - V_{j,t}\cos\theta_{j,t}) - b_{ij}(V_{j,t}\sin\theta_{i,t} - V_{j,t}\sin\theta_{j,t}) \tag{12}$$

$$I_{M_{ij,t}} = g_{ij}(V_{i,t}\sin\theta_{i,t} - V_{j,t}\sin\theta_{j,t}) + b_{ij}(V_{j,t}\cos\theta_{i,t} - V_{j,t}\cos\theta_{j,t}) \tag{13}$$

where Equations (4) and (5) represent the active and reactive power balance at IOP, respectively, with consideration for different power sources. The active and reactive power flow through the branches at IOP are shown with constraints (6) and (7), respectively. The contribution of the substation for active and reactive power supply is limited by

Equations (8) and (9), respectively. The bus voltage limits are represented with Equation (10), while Equations (11)–(13) show the limits on the transmission lines.

3.1.2. Power Flow Constraints at MLP

As stated, this paper considers the power flow constraints at IOP and MLP simultaneously. The power flow constraints at MLP are given below:

$$\hat{P}^{G}_{i,t} + P^{WF}_{i,t} + P^{CH}_{i,t} - \hat{P}^{D}_{i,t} - P^{DICCH}_{i,t} = \sum_{j} (\delta^{L}_{ij,t} \times \hat{P}_{ij,t}) \tag{14}$$

$$\hat{Q}^{G}_{i,t} + Q^{WF}_{i,t} - \hat{Q}^{D}_{i,t} = \sum_{j} (\delta^{L}_{ij,t} \times \hat{Q}_{ij,t}) \tag{15}$$

$$\hat{P}_{ij,t} = \hat{V}^{2}_{i,t} g_{ij} - \hat{V}_{i,t}\hat{V}_{j,t}(g_{ij}\cos\hat{\theta}_{ij,t} + b_{ij}\sin\hat{\theta}_{ij,t}) \tag{16}$$

$$\hat{Q}_{ij,t} = -\hat{V}^{2}_{i,t} g_{ij} - \hat{V}_{i,t}\hat{V}_{j,t}(g_{ij}\sin\hat{\theta}_{ij,t} - b_{ij}\cos\hat{\theta}_{ij,t}) \tag{17}$$

$$\hat{P}^{D}_{i,t} = (1 + K_{D,i}\ \lambda)\ P^{D}_{i,t} \tag{18}$$

$$\hat{Q}^{D}_{i,t} = (1 + K_{D,i}\lambda)(Q^{D}_{i,t}) \tag{19}$$

$$\hat{P}^{G}_{s,t} = \min\left(P^{\max}_{G}, (1 + K_{G,s}\lambda)P^{G}_{s,t}\right) \tag{20}$$

$$\begin{cases} P^{\min}_{sub} \le \hat{P}^{G}_{s,t} \le P^{\max}_{sub} & ;\forall i \in N_s \\ 0 & ;\text{otherwise} \end{cases} \tag{21}$$

$$\begin{cases} Q^{\min}_{sub} \le \hat{Q}^{G}_{s,t} \le Q^{\min}_{sub} & ;\forall i \in N_s \\ 0 & ;\text{otherwise} \end{cases} \tag{22}$$

$$V^{\min}_{i} \le \hat{V}_{i,t} \le V^{\max}_{i} \tag{23}$$

$$\delta^{L}_{ij,t}(\hat{I}^{2}_{R_{ij,t}} + \hat{I}^{2}_{M_{ij,t}}) \le \hat{I}^{2}_{MAX_{ij}} \tag{24}$$

$$\hat{I}_{R_{ij,t}} = g_{ij}(\hat{V}_{i,t}\cos\hat{\theta}_{i,t} - \hat{V}_{j,t}\cos\hat{\theta}_{j,t}) - b_{ij}(\hat{V}_{j,t}\sin\hat{\theta}_{i,t} - \hat{V}_{j,t}\sin\hat{\theta}_{j,t}) \tag{25}$$

$$\hat{I}_{M_{ij,t}} = g_{ij}(\hat{V}_{i,t}\sin\hat{\theta}_{i,t} - \hat{V}_{j,t}\sin\hat{\theta}_{j,t}) + b_{ij}(\hat{V}_{j,t}\cos\hat{\theta}_{i,t} - \hat{V}_{j,t}\cos\hat{\theta}_{j,t}) \tag{26}$$

$$\lambda \ge \lambda_{des} > 0 \tag{27}$$

where constraints (14)–(17) represent the load balance and power flow through the branches at MLP, respectively. The active and reactive power increase pattern of loads from IOP to MLP are given by Equations (18) and (19), respectively. The substation active power is increased to cover the load increase, as shown in Equation (20). Constraints (21)–(26) represent the physical and operational limits of the substation and transmission lines. The desired loading parameter is defined by Equation (27).

3.1.3. WF's Capacity Limit

In this study, the optimal locations of *WFs* are defined based on their effect on the stability of the network. A discrete variable-based formulation is introduced for the *WFs* allocation, with consideration for the power output of the *WFs* in IOP and MLP.

$$\forall i \in N_{WF}, \forall t \in N_t$$

$$\begin{cases} 0 \le P^{WF}_{i,t} \le \vartheta^{WF}_{i} \times \eta^{WF}_{i} \times P^{WF,sd}_{i} \times CF^{WF}_{i,t} & ;\forall i \in N_{WF} \\ 0 & ;otherwise \end{cases} \tag{28}$$

$$\begin{cases} -tg(\varphi_{lead}) \times P^{WF}_{i,t} \times \vartheta^{WF}_{i} \le Q^{WF}_{i,t} \le \vartheta^{WF}_{i} \times tg(\varphi_{lag}) \times P^{WF}_{i,t} & ;\forall i \in N_{WF} \\ 0 & ;otherwise \end{cases} \tag{29}$$

$$\sum_{i \in N_b} \vartheta_i^{WF} \leq N_{\max}^{WF} \tag{30}$$

$$\eta_i^{WF} \leq \eta_i^{WF,\max} \tag{31}$$

where constraints (28) and (29) represent the active and reactive power limit of *WFs*, respectively. The parameter $CF_{i,t}^{WF}$ is defined here to specify the expected power output of *WF* installed in bus i at time t. The binary variable ϑ_i^{WF} is introduced to define the optimal location of *WFs* based on the security constraint. Constraint (30) limits the number of *WFs* which could be installed in the network. The uncertainty of wind power generation has not been considered in this study. However, it can be considered as a potential future work. The uncertainty of wind power generation can affect the system security and the network reconfiguration.

3.1.4. ESS Capacity

The charge/discharge power of *ESS* is an important variable affecting the proposed optimization problem. Due to the effect of *ESS* on the operational and economic performance of the optimization, their location should be defined for optimal operation of the DN. The *ESS* model is represented below:

$$\forall i \in N_{ESS}, \forall t \in N_t$$

$$\begin{cases} 0 \leq P_{i,t}^{CH} \leq \gamma_{i,t}^{ch} \times P_{i,t}^{ch,\max} \times \vartheta_i^{ESS} & ; \forall i \in N_{ESS} \\ 0 & ; otherwise \end{cases} \tag{32}$$

$$\begin{cases} 0 \leq P_{i,t}^{DISCH} \leq \gamma_{i,t}^{disch} \times p_{i,t}^{disch,\max} \times \vartheta_i^{WF} & ; \forall i \in N_{ESS} \\ 0 & ; otherwise \end{cases} \tag{33}$$

$$\gamma_{i,t}^{ch} + \gamma_{i,t}^{disch} \leq 1 \ , \ \ (\gamma_{i,t}^{disch}, \gamma_{i,t}^{ch} \in \{0,1\}) \tag{34}$$

$$SOC_{i,t}^{ESS} = SOC_{i,t}^{ESS} + \Delta t.(p_{i,t}^{CH} \eta_{i,t}^{ch} - p_{i,t}^{DISCH} / \eta_{i,t}^{dch})0 \tag{35}$$

$$SOC_i^{\min} \times \eta_i^{ESS} \leq SOC_{i,t}^{ESS} \leq SOC_i^{\max} \times \eta_i^{ESS} \tag{36}$$

$$\sum_{i \in \Omega_b} \vartheta_i^{ESS} \leq N_{\max}^{ESS} \tag{37}$$

where the upper and lower bands of the *ESS* charge and discharge power are shown in Equations (32) and (33). Constraint (34) prevents the simultaneous charge and discharge of *ESSs*. Constraint (35) shows the state of charge (*SOC*) of the *ESSs*, which is limited by Equation (36). Finally, Equation (37) limits the number of *ESSs* that could be installed in the network.

3.1.5. Topology Reconfiguration

The network reconfiguration can be defined based on the concept of graph theory, which defines a tree as a connected graph without any loop [27]. In radial distribution networks, two important conditions apply: (1) the tree topology which requires the graph theory condition, and (2) connectivity of system buses to the substation. The first condition can be satisfied if the number of closed switches in the network will be equal to the number of nodes minus one. This concept is mathematically expressed as:

$$\sum_{ij \in N_b} \delta_{ij,t}^{L} = 2 \times (n_b - 1) \tag{38}$$

$$\delta_{ij,t}^{L} = \delta_{ji,t}^{L} \qquad \forall i, j \in N_b, t \in N_t \tag{39}$$

The power balance equations satisfy the second condition, where there is a power flow from the substation to each bus at each hour. Unlike other studies, in this study, the power balance equations are satisfied for both IOP and MLP, simultaneously.

4. Simulation Parameters

The IEEE 33-bus distribution network [28] is used in simulating the proposed model. This system consists of 32 sectionalizing switches and 5 tie switches, and the voltage level of all system buses is 12.66 kV. The active and reactive system load is 3.715 MW and 2.3 MVaR, respectively. Figure 2 depicts the distribution network in its initial configuration. To illustrate the impact of voltage stability on the optimal allocation of WFs, the system load demand is increased by a factor of 1.2. Furthermore, it is assumed that a maximum of 0.5 MW of ESS can be installed in the distribution network. The data of the IEEE 33-bus distribution network used in the simulation is given in [29]. On a personal computer equipped with an Intel i7 processor running at 3.00 GHz with 8 gigabytes of random-access memory, the proposed problem is simulated as a mixed integer non-linear programming (MINLP) problem in the general algebraic modeling system (GAMS) [30] environment using a standard branch and bound solver. The model is solved with SBB in GAMS, which uses a standard branch and bond algorithm to solve the problem. A 24 h operation period is considered for the simulation. It should be noted that the numbers representing the time periods do not represent the time of day. Figure 3 illustrates the pattern of load demand on the system, as well as the price profile of electricity at each hour [31]. Tables 3 and 4, respectively, provide information about the capacity factor of the *WFs* [31] and the characteristics of the *ESSs* [32] used in the simulation. Furthermore, it has been assumed in the simulation that the LM should be 0.15. The maximum number of three *WFs*, each with eight wind turbines and a capacity of 250 kW and two *ESS*, each with a capacity of 0.5 MW, are considered for installation in the distribution network.

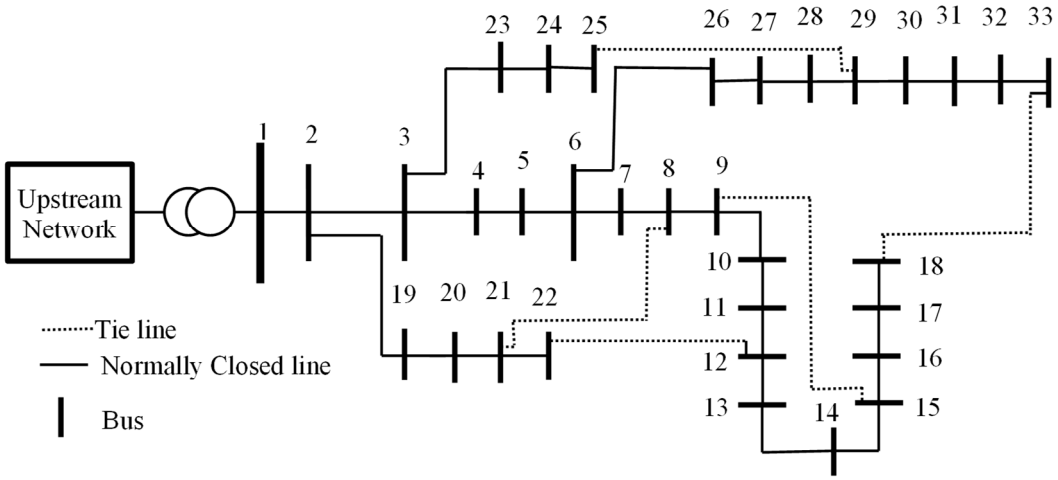

Figure 2. Single line diagram of the IEEE 33-bus system [28] in the initial configuration.

Table 3. Capacity factor of *WFs* in each hour [31].

1	2	3	4	5	6	7	8	9	10	11	12
0.08	0.09	0.12	0.26	0.36	0.59	0.65	0.59	0.49	0.55	0.77	0.72
13	14	15	16	17	18	19	20	21	22	23	24
0.83	0.92	0.97	1.00	0.83	0.65	0.65	0.56	0.57	0.56	0.72	0.84

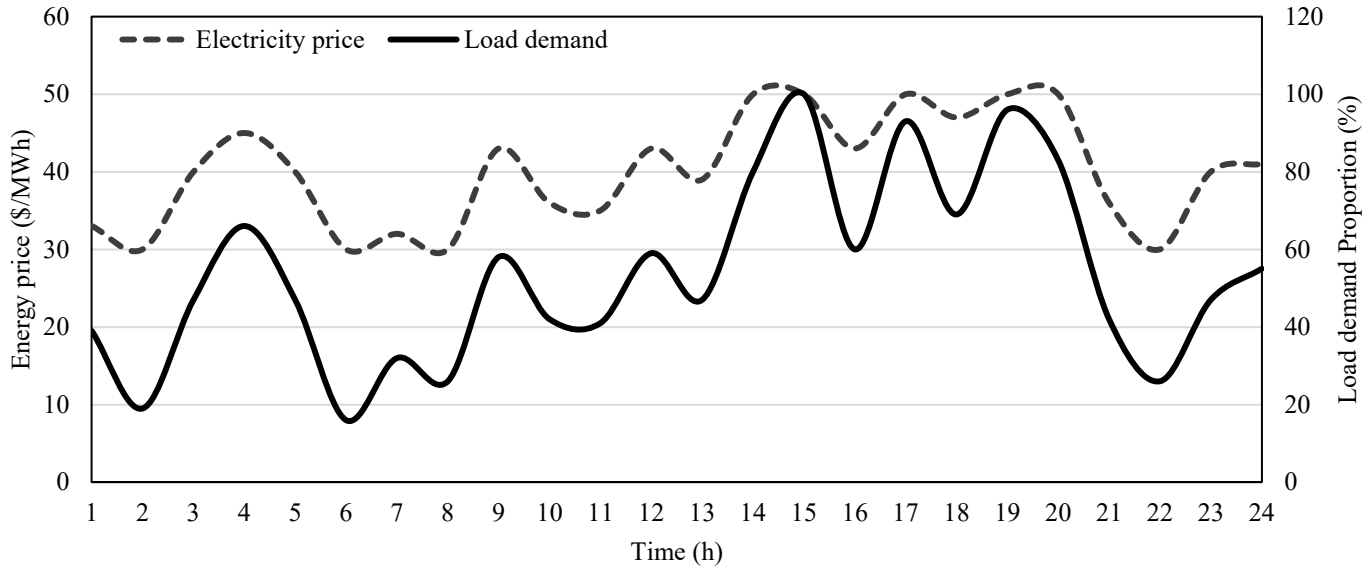

Figure 3. System load demand profile and electricity price variation [31].

Table 4. Characteristics of ESSs [32].

$P_{i,t}^{ch,\max}(MW)$	$P_{i,t}^{dich,\max}(MW)$	$\eta_{i,t}^{ch}$	$\eta_{i,t}^{dich}$	$SOC_i^{\max}$	$SOC_i^{\min}$
0.20	0.20	0.88	0.88	1.00	0.10

To demonstrate the link between the constraints of the voltage stability and the network reconfiguration, the following two case studies are considered. In the first case study (Case Study I), the model considers the optimal reconfiguration of the network. However, in the second case study (Case Study II), the proposed model neglects the optimal reconfiguration. Neglecting the reconfiguration can be done by ignoring Equations (36)–(38) from the model. A sensitivity analysis is carried out to investigate how the distribution network security constraints influence the optimal allocation of WFs and ESSs, as well as the hourly reconfiguration of the distribution network. Furthermore, the effects of contingency situations are investigated.

5. Results and Discussion

The simulation findings that describe the linkage between HDNR, network security, and the allocation of *WFs* and *ESSs* will be examined in this section. The values of the objective function in Case Study I and Case Study II are USD 2443.80 and USD 2437.54, respectively. Comparing these two values reveals that GenCo's costs have gone up by a marginal amount. This relatively minor increase in cost is seen as a security cost, which suggests that simultaneous consideration of both distribution network security restrictions and HDNR gives rise to an increase in purchase costs. It is important to note that this increase in the security cost only applies to a day of operation considered in the simulation; hence, it is possible that this cost will drastically increase in the long-term operation of the distribution network.

These two case studies also demonstrate that the optimal allocation of the *WTs* and *ESSs* is affected by the optimal HDNR. The simulations for the two case studies were conducted for the initial configuration shown in Figure 4.

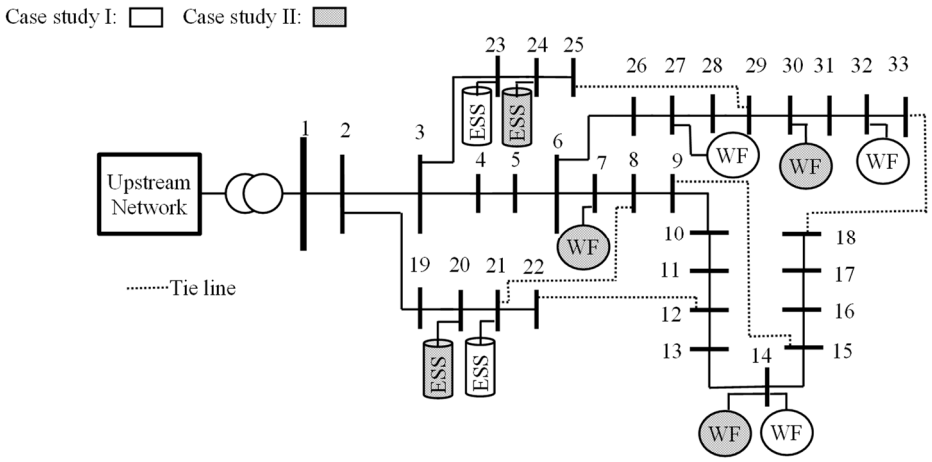

Figure 4. Optimal location of *WFs* and *ESSs* for Case Study I and Case Study II.

Figure 5 shows the optimal HDNR of Case Study I. This figure shows how the network's configuration can be changed throughout the day. This result demonstrates the importance of optimal HDNR in the future smart grid.

Figure 6 shows the utilized wind power in the distribution network for the two case studies. The evolutions of the *SOC* of the *ESSs* for the two case studies are given in Figure 7. From these two figures, it can be seen that the greatest injection of wind power to the distribution network happens during the peak hours (from 3 to 8 p.m.), and the *ESSs* have been discharged at a high rate during these peak hours. Figure 6 also shows that in Case Study I, the amount of utilized wind power in the distribution network is reduced, and this happens as a result of the simultaneous consideration of security constraints and HDNR.

5.1. Sensitivity Analysis

A sensitivity analysis is performed for different amounts of desired LM, with and without accounting for LM constraints. Neglecting Equations (14)–(27) will lead to ignoring the LM constraints in the problem. The aim of this sensitivity analysis is to demonstrate the effect of LM constraints on the proposed problem. Table 5 shows the number of switches opened in 24 h for the proposed model, with and without LM constraints for various levels of desired LM, demonstrating that LM limitations have a significant impact on network reconfiguration. This means that as the LM increases, the network is changed every hour to operate the distribution network securely. Note that the numbers in this table represent the bus number.

For example, in the presence of intermittent wind generation, the network configuration for the desired LM of 0.15 is the secured configuration in each hour. Table 6 gives the optimal location of the *WFs* and *ESSs* for the analysis. It is evident from this table that the optimal location and size of *WFs* and *ESSs* are affected by security of the system. This means that consideration for security constraints is an important factor in the optimal allocation of DERs. Furthermore, it can be shown in Figure 8 that the values for the objective function of the GenCo's cost for increasing the desired LM are also increased. This means that the GenCo should spend more money to guarantee the safe operation of the system from the point of view of voltage stability.

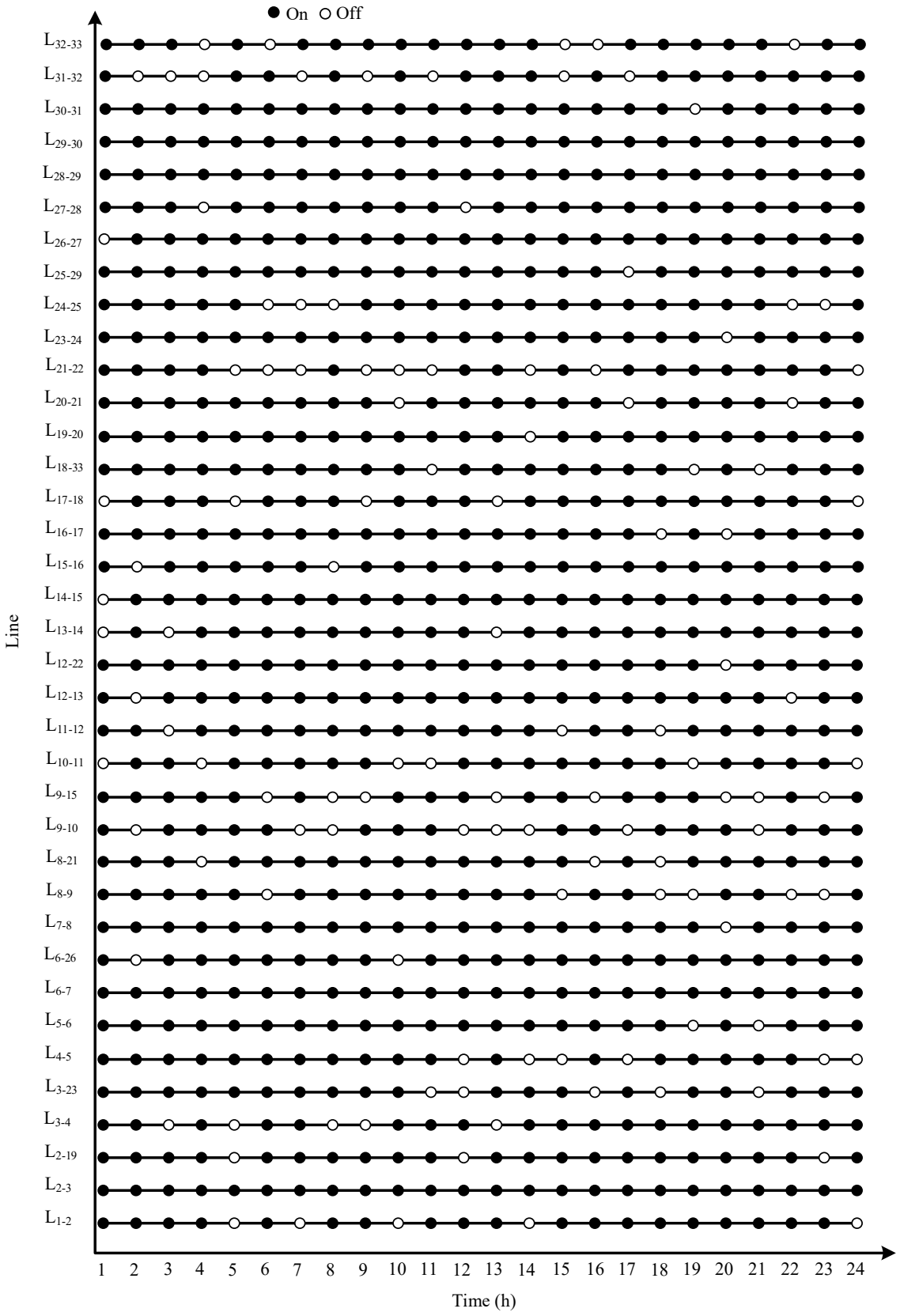

Figure 5. Case Study I hourly configuration of network, when network security and optimal allocation of *WFs* and *ESSs* are considered.

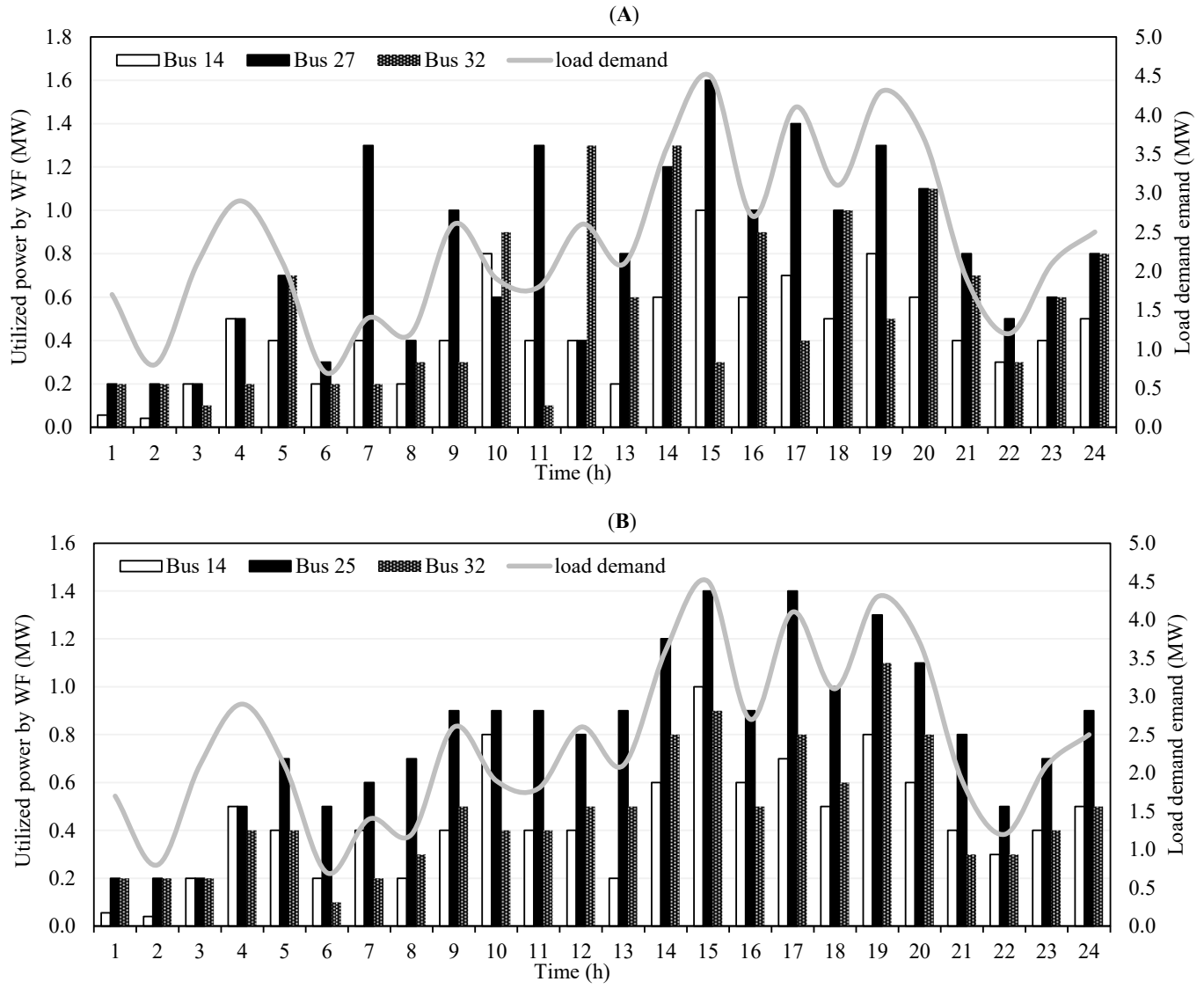

Figure 6. Utilized wind power for (**A**), Case Study I, and (**B**), Case Study II.

5.2. Contingency Analysis

As previously indicated, the accurate determination of LM could ensure the security of the distribution network in terms of voltage stability. To highlight this important role of LM, a simulation has been performed, assuming that a distribution network line is destroyed by a natural disaster or a man-made problem. More precisely, it was assumed in the IEEE 33-bus DN that the line between buses 6 and 26 is affected. The operation of the distribution network is then investigated under the following two conditions, C1: contingency condition, and C2: normal condition. Figure 9 shows the cumulative utilized wind power of *WFs* under these two conditions. This figure clearly illustrates the critical importance of *WFs* to cover distribution network loads and prevent load curtailment in contingency situations. On the other hand, the simulation reveals that the values of the cost function in these two conditions are USD 2461.43 and USD 2443.80, respectively. Comparing these two values demonstrates the increase in the GenCo's costs as a result of the contingency condition. The last operational aspect to investigate under these two conditions is the security of the distribution network under study. For this purpose, the P-V curve of bus 24 at hour 15 is plotted under both operational conditions, C1 and C2 (Figure 10). This figure shows that the LM of the system drops significantly under the contingency condition, providing insight into the security of distribution network in both

conditions. The distribution network may undergo a critical operation leading to a failure if at least a minimal value for LM is not evaluated under the contingency condition. Even though the distribution network's LM drops dramatically under the contingency condition, the value of LM is still appropriate for a secured operation of the distribution network.

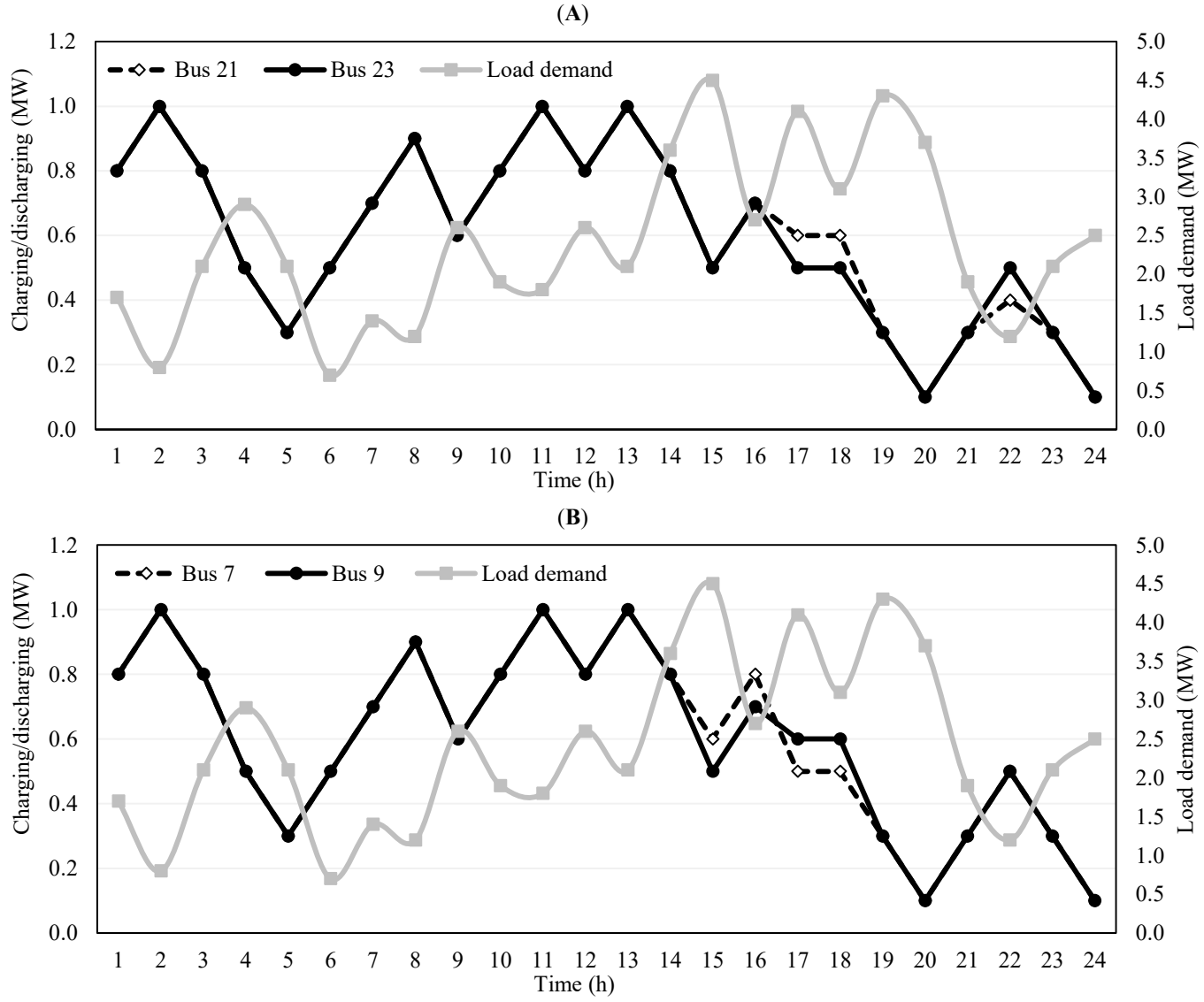

Figure 7. Charging/discharging pattern of *ESSs* for (**A**), Case Study I, and (**B**), Case Study II.

Table 5. Optimal configuration of network, with and without LM constraints, in 24 h.

Time (h)	Potentially Opened Lines			
	Without LM Constraints	**With LM Constraints (λ_{des} = 0.10)**	**With LM Constraints (λ_{des} = 0.15)**	**With LM Constraints (λ_{des} = 0.20)**
1	$L_{4\text{-}5}$, $L_{7\text{-}8}$, $L_{9\text{-}10}$, $L_{13\text{-}14}$, $L_{32\text{-}33}$	$L_{6\text{-}26}$, $L_{9\text{-}15}$, $L_{10\text{-}11}$, $L_{19\text{-}20}$, $L_{32\text{-}33}$	$L_{10\text{-}11}$, $L_{13\text{-}14}$, $L_{14\text{-}15}$, $L_{17\text{-}18}$, $L_{26\text{-}27}$	$L_{2\text{-}3}$, $L_{10\text{-}11}$, $L_{14\text{-}15}$, $L_{16\text{-}17}$, $L_{25\text{-}29}$
2	$L_{9\text{-}10}$, $L_{9\text{-}15}$, $L_{13\text{-}14}$, $L_{14\text{-}15}$, $L_{24\text{-}25}$	$L_{7\text{-}8}$, $L_{10\text{-}11}$, $L_{13\text{-}14}$, $L_{14\text{-}15}$, $L_{16\text{-}17}$	$L_{3\text{-}4}$, $L_{9\text{-}10}$, $L_{12\text{-}13}$, $L_{14\text{-}15}$, $L_{31\text{-}32}$	$L_{4\text{-}5}$, $L_{9\text{-}15}$, $L_{11\text{-}12}$, $L_{12\text{-}13}$, $L_{27\text{-}28}$
3	$L_{6\text{-}7}$, $L_{10\text{-}11}$, $L_{14\text{-}15}$, $L_{21\text{-}22}$, $L_{30\text{-}31}$	$L_{6\text{-}26}$, $L_{9\text{-}10}$, $L_{9\text{-}15}$, $L_{31\text{-}32}$, $L_{32\text{-}33}$	$L_{3\text{-}4}$, $L_{11\text{-}12}$, $L_{13\text{-}14}$, $L_{31\text{-}32}$, $L_{32\text{-}33}$	$L_{4\text{-}5}$, $L_{6\text{-}7}$, $L_{9\text{-}15}$, $L_{10\text{-}11}$, $L_{31\text{-}32}$

Table 5. *Cont.*

Time (h)	Potentially Opened Lines			
	Without LM Constraints	**With LM Constraints (λ_{des} = 0.10)**	**With LM Constraints (λ_{des} = 0.15)**	**With LM Constraints (λ_{des} = 0.20)**
4	L_{6-7}, L_{9-10}, L_{14-15}, L_{21-22}, L_{31-32}	L_{3-4}, L_{9-10}, L_{12-22}, L_{18-33}, L_{31-32}	L_{8-21}, L_{10-11}, L_{27-28}, L_{31-32}, L_{32-33}	L_{8-9}, L_{10-11}, L_{12-22}, L_{31-32}, L_{32-33}
5	L_{8-21}, L_{12-22}, L_{13-14}, L_{15-16}, L_{23-24}	L_{3-23}, L_{8-9}, L_{8-21}, L_{12-13}, L_{17-18}	L_{1-2}, L_{2-19}, L_{3-4}, L_{17-18}, L_{21-22}	L_{4-5}, L_{6-26}, L_{8-21}, L_{9-15}, L_{13-14}
6	L_{3-23}, L_{4-5}, L_{10-11}, L_{15-16}, L_{30-31}	L_{5-6}, L_{6-7}, L_{10-11}, L_{16-17}, L_{24-25}	L_{8-9}, L_{9-15}, L_{21-22}, L_{24-25}, L_{32-33}	L_{1-2}, L_{5-6}, L_{9-15}, L_{12-22}, L_{18-33}
7	L_{12-22}, L_{16-17}, L_{20-21}, L_{26-27}, L_{30-31}	L_{4-5}, L_{10-11}, L_{16-17}, L_{21-22}, L_{30-31}	L_{1-2}, L_{9-10}, L_{9-15}, L_{15-16}, L_{24-25}	L_{1-2}, L_{4-5}, L_{6-7}, L_{11-12}, L_{18-33}
8	L_{1-2}, L_{3-23}, L_{12-22}, L_{16-17}, L_{20-21},	L_{2-19}, L_{3-23}, L_{4-5}, L_{15-16}, L_{30-31}	L_{3-4}, L_{9-10}, L_{9-15}, L_{15-16}, L_{24-25}	L_{1-2}, L_{2-19}, L_{3-4}, L_{11-12}, L_{32-33}
9	L_{3-23}, L_{6-7}, L_{12-22}, L_{13-14}, L_{16-17}	L_{1-2}, L_{3-4}, L_{6-26}, L_{9-10}, L_{15-16}	L_{3-4}, L_{9-15}, L_{17-18}, L_{21-22}, L_{31-32}	L_{2-3}, L_{4-5}, L_{10-11}, L_{12-13}, L_{18-33}
10	L_{8-21}, L_{9-15}, L_{11-12}, L_{17-18}, L_{21-22}	L_{7-8}, L_{8-21}, L_{10-11}, L_{16-17}, L_{6-7}	L_{1-2}, L_{6-26}, L_{10-11}, L_{20-21}, L_{21-22}	L_{2-3}, L_{6-7}, L_{10-11}, L_{19-20}, L_{32-33}
11	L_{5-6}, L_{7-8}, L_{12-22}, L_{20-21}, L_{23-24}	L_{10-11}, L_{13-14}, L_{14-15}, L_{20-21}, L_{25-29}	L_{3-23}, L_{10-11}, L_{18-33}, L_{21-22}, L_{31-32}	L_{1-2}, L_{2-19}, L_{4-5}, L_{9-10}, L_{18-33}
12	L_{6-26}, L_{8-21}, L_{12-13}, L_{12-22}, L_{16-17}	L_{2-3}, L_{11-12}, L_{12-13}, L_{14-15}, L_{15-16}	L_{2-19}, L_{3-23}, L_{4-5}, L_{9-10}, L_{27-28}	L_{3-23}, L_{6-7}, L_{8-21}, L_{20-21}, L_{32-33}
13	L_{5-6}, L_{9-15}, L_{12-22}, L_{16-17}, L_{23-24}	L_{3-23}, L_{7-8}, L_{8-21}, L_{16-17}, L_{30-31}	L_{3-4}, L_{9-10}, L_{9-15}, L_{13-14}, L_{17-18}	L_{4-5}, L_{6-26}, L_{11-12}, L_{12-13}, L_{23-24}
14	L_{9-15}, L_{10-11}, L_{12-13}, L_{15-16}, L_{23-24}	L_{4-5}, L_{6-7}, L_{9-10}, L_{12-22}, L_{16-17}	L_{1-2}, L_{4-5}, L_{9-10}, L_{19-20}, L_{21-22}	L_{4-5}, L_{6-7}, L_{10-11}, L_{13-14}, L_{25-29}
15	L_{6-7}, L_{6-26}, L_{8-21}, L_{20-21}, L_{23-24}	L_{3-4}, L_{19-20}, L_{21-22}, L_{30-31}, L_{32-33}	L_{4-5}, L_{8-9}, L_{11-12}, L_{31-32}, L_{32-33}	L_{5-6}, L_{6-7}, L_{11-12}, L_{13-14}, L_{23-24}
16	L_{5-6}, L_{6-7}, L_{13-14}, L_{16-17}, L_{20-21}	L_{6-7}, L_{6-26}, L_{10-11}, L_{16-17}, L_{21-22}	L_{3-23}, L_{8-21}, L_{9-15}, L_{21-22}, L_{32-33}	L_{2-19}, L_{3-23}, L_{4-5}, L_{8-9}, L_{18-33}
17	L_{6-26}, L_{8-9}, L_{12-22}, L_{13-14}, L_{16-17}	L_{6-26}, L_{8-21}, L_{9-10}, L_{21-22}, L_{23-24}	L_{4-5}, L_{9-10}, L_{20-21}, L_{25-29}, L_{31-32}	L_{1-2}, L_{4-5}, L_{11-12}, L_{18-33}, L_{19-20}
18	L_{6-26}, L_{11-12}, L_{20-21}, L_{21-22}, L_{23-24}	L_{7-8}, L_{12-22}, L_{18-33}, L_{24-25}, L_{31-32}	L_{3-23}, L_{8-9}, L_{8-21}, L_{11-12}, L_{16-17}	L_{1-2}, L_{2-19}, L_{12-13}, L_{21-22}, L_{32-33}
19	L_{3-4}, L_{9-10}, L_{12-22}, L_{14-15}, L_{15-16}	L_{3-23}, L_{9-10}, L_{17-18}, L_{21-22}, L_{30-31}	L_{5-6}, L_{8-9}, L_{10-11}, L_{18-33}, L_{30-31}	L_{2-3}, L_{10-11}, L_{16-17}, L_{18-33}, L_{26-27}
20	L_{3-23}, L_{9-15}, L_{10-11}, L_{16-17}, L_{21-22}	L_{3-23}, L_{4-5}, L_{11-12}, L_{17-18}, L_{30-31}	L_{7-8}, L_{9-15}, L_{12-22}, L_{16-17}, L_{23-24}	L_{4-5}, L_{7-8}, L_{8-9}, L_{11-12}, L_{13-14}
21	L_{3-23}, L_{7-8}, L_{12-22}, L_{16-17}, L_{30-31}	L_{4-5}, L_{9-10}, L_{24-25}, L_{31-32}, L_{32-33}	L_{3-23}, L_{5-6}, L_{9-10}, L_{9-15}, L_{18-33}	L_{1-2}, L_{3-4}, L_{9-10}, L_{18-33}, L_{31-32}
22	L_{8-9}, L_{12-22}, L_{13-14}, L_{16-17}, L_{20-21}	L_{7-8}, L_{8-21}, L_{10-11}, L_{13-14}, L_{16-17}	L_{8-9}, L_{12-13}, L_{20-21}, L_{24-25}, L_{32-33}	L_{2-19}, L_{3-23}, L_{4-5}, L_{18-33}, L_{21-22}
23	L_{3-23}, L_{6-7}, L_{6-26}, L_{8-9}, L_{16-17}	L_{6-26}, L_{8-9}, L_{11-12}, L_{16-17}, L_{20-21}	L_{2-19}, L_{4-5}, L_{8-9}, L_{24-25}, L_{9-15}	L_{4-5}, L_{18-33}, L_{20-21}, L_{21-22}, L_{30-31}
24	L_{3-23}, L_{4-5}, L_{7-8}, L_{8-21}, L_{13-14}	L_{7-8}, L_{8-9}, L_{11-12}, L_{14-15}, L_{24-25}	L_{1-2}, L_{4-5}, L_{10-11}, L_{17-18}, L_{21-22}	L_{1-2}, L_{9-10}, L_{12-13}, L_{18-33}, L_{31-32}

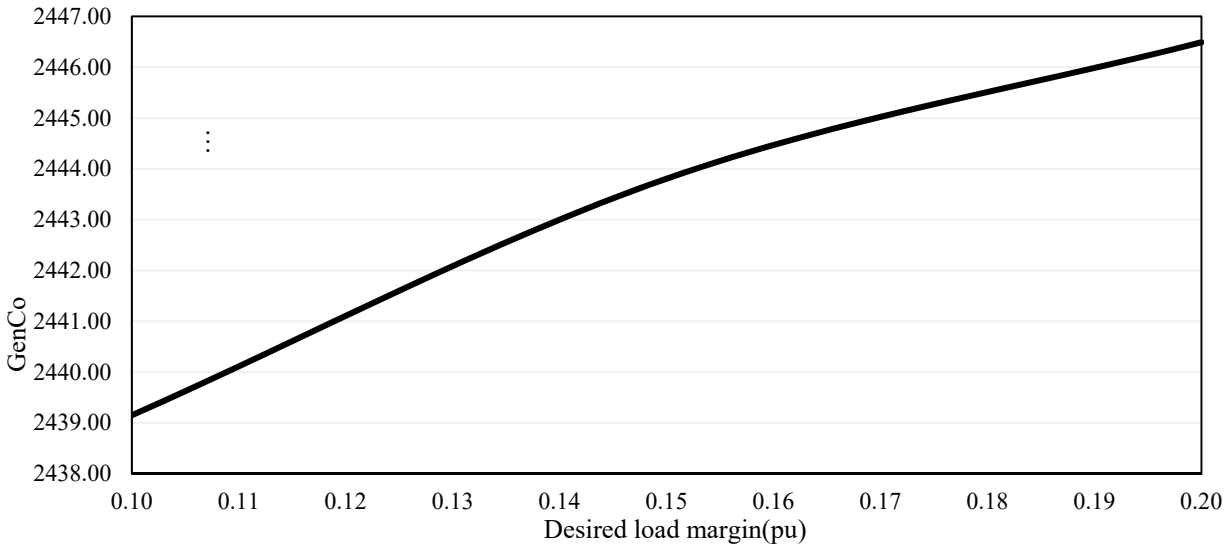

Figure 8. GenCo's cost of purchasing power from the grid and the *WFs*, based on the variation of desired LM.

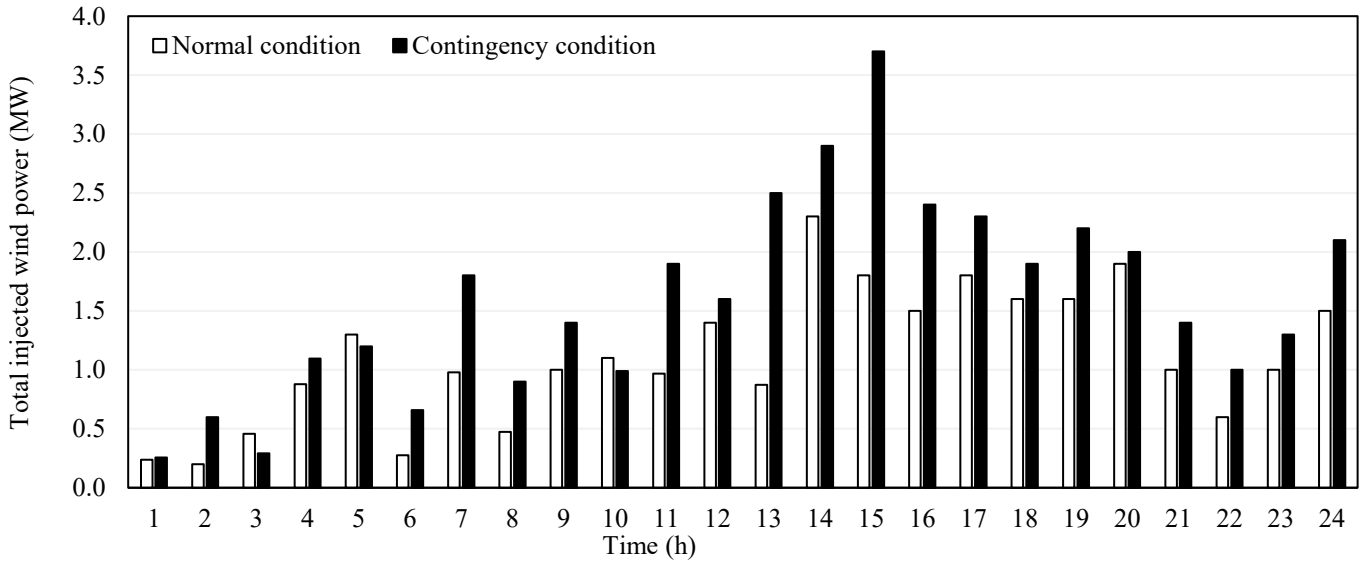

Figure 9. Total utilized power of WFs for normal and contingency conditions.

Table 6. Optimal location of *WFs* and *ESS*, with and without LM constraints.

Model State	*WF* (Bus No.)	Number of Wind Turbines	Cumulative Capacity (MW)	ESS (Bus No.)
(a) W/O LM constraints				
	14	5	1.25	
	25	6	1.5	7, 9
	32	5	1.25	
(b) W LM constraints (λ_{des} = 0.10)				
	14	6	1.5	
	30	7	1.6	5, 30
	32	2	0.5	

Table 6. *Cont.*

Model State	*WF* (Bus No.)	Number of Wind Turbines	Cumulative Capacity (MW)	ESS (Bus No.)
(c) W LM constraints (λ_{des} = 0.15)	14	4	1	
	27	7	1.75	21, 23
	32	6	1.5	
(d) W LM constraints (λ_{des} = 0.20)	18	8	2	
	25	6	1.5	9, 25
	32	2	0.5	

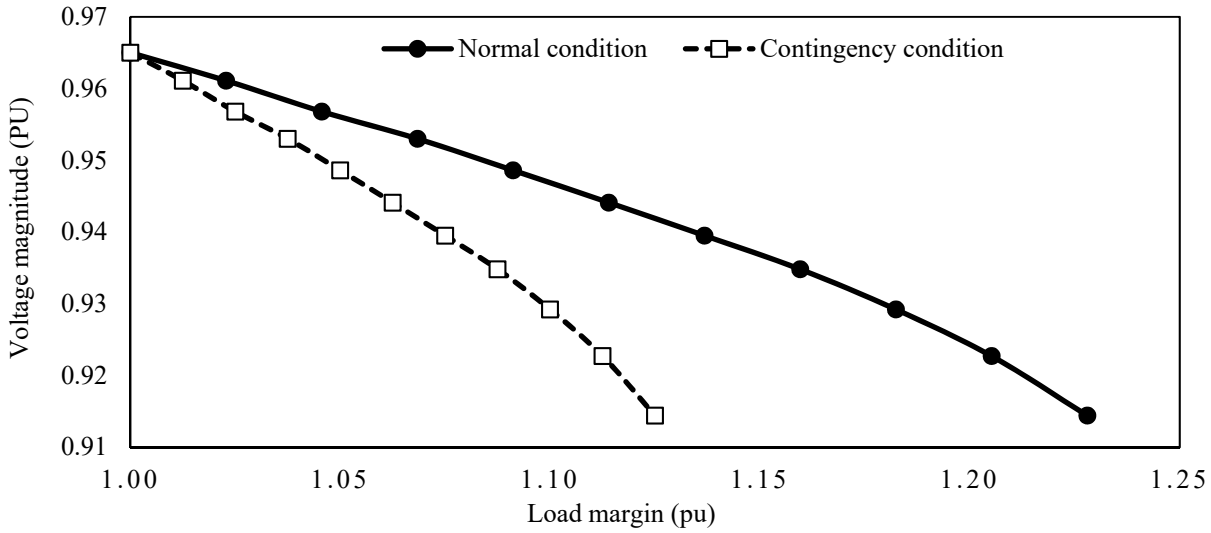

Figure 10. Voltage profile of Bus 24 for different conditions.

6. Conclusions

This study presents a secure reconfiguration method for distribution networks in the presence of wind farms and energy storage systems under normal and emergency conditions. By modeling voltage stability with LM constraints and optimizing the DNR schedule to maintain a desired level of LM, the proposed model ensures the security of the distribution network during the reconfiguration process and emergency situations. Furthermore, the proposed model implements an hourly switch status schedule to optimize the allocation of *WFs* and *ESSs*, while ensuring the secure operation of the distribution network. The results of the study, conducted on an IEEE 33-bus distribution system indicate the importance of LM constraints in hourly reconfiguration of distribution networks and in determining the optimal allocation of *WFs* and *ESSs*. Additionally, the study concludes that proper LM guarantees the security of the system under emergency conditions and that ESSs can be optimally scheduled to control *WF* power output and cover system loads. Future research could consider the role of plug-in electric vehicles in supplying system load demand, especially during critical emergencies, and contingencies in long-term planning, as they may impact optimization procedures.

Author Contributions: Conceptualization, S.N.; methodology, S.N.; software, S.N.; validation, S.N., A.A. (Arman Alahyari) and A.A. (Adib Allahhham); formal analysis, S.N.; resources, A.A. (Arman Alahyari) and K.A.; writing—original draft preparation, S.N.; writing—review and editing, S.N., A.A. (Arman Alahyari) and A.A. (Adib Allahhham); supervision, A.A. (Adib Allahhham) and K.A.; project administration, A.A. (Adib Allahhham) and K.A.; funding acquisition, A.A. (Adib Allahham) and K.A. All authors have read and agreed to the published version of the manuscript.

Funding: This paper was supported by the Royal Academy of Engineering through the Engineering X Transforming Systems through the Partnership Program, Project No. TSP2021/100334.

Data Availability Statement: Data are contained within the article.

Conflicts of Interest: The authors declare no conflict of interest.

Nomenclature

Indices	
i, j	Index for system buses
l	Index for transmission lines
t	Index for times
Sets	
N_s	Set of substations connecting the distribution network to the upstream networks
N_l	Set of transmission lines
N_b	Set of system buses
N_{ESS}	Set of ESS installed buses
N_{WF}	Set of WF installed buses
N_t	Set of times
Variables and Parameters	
$P^G_{i,t}/Q^G_{i,t}$	Active/reactive power injected from substation to bus i at time t at *IOP* (pu)
$P^D_{i,t}/Q^D_{i,t}$	Active/reactive power consumption of load connected to bus i at time t at *IOP* (pu)
$\hat{P}^G_{i,t}/\hat{Q}^G_{i,t}$	Active/reactive power injected from substation to bus i at time t at *MLP* (pu)
$\hat{P}^D_{i,t}/\hat{Q}^D_{i,t}$	Active/reactive power consumption of load connected to bus i at time t at *MLP* (pu)
$P_{ij,t}/Q_{ij,t}$	Active/reactive power flow that leaves node i toward node j at time t at *IOP* (pu)
$\hat{P}_{ij,t}/\hat{Q}_{ij,t}$	Active/reactive power flow that leaves node i toward node j at time t at *MLP* (pu)
δ^L_{ij}	Binary variable for the line between buses i and j (1 = connected, 0 = disconnected)
ϑ^{ESS}_i	Binary variable for location of *ESS* installed at bus i (1 = installed, 0 = otherwise)
ϑ^{WF}_i	Binary variable for location of *WF* installed at bus i (1 = installed, 0 = otherwise)
$CF^{WF}_{i,t}$	Capacity factor of *WF* installed at bus i at time t
$\eta^{ch/dch}_{i,t}$	Charging/discharging efficiencies of *ESS*s
$\gamma^{ch/dch}_{i,t}$	Charging/discharging decisions of *ESS*s (1 = allowed, 0 = not allowed)
$P^{CH/DISCH}_{i,t}$	Charge/discharge power of *ESS* installed in bus i at time t (pu)
g_{ij}/b_{ij}	Conductance/susceptance of line between buses i and j (pu)
$I_{l,t}$	Current flow through line l at time t (pu)
λ_{des}	Desired loading margin (pu)
C^{pur}_t	Electricity price cost at time t (USD/MWh)
$I_{M_{ij,t}}$	Imaginary current flow component of branch between buses i and j at time t at *IOP* (pu)
$\hat{I}_{M_{ij,t}}$	Imaginary current flow component of branch between buses i and j at time t at *MLP* (pu)
$(P/Q)^{WF}_{i,t}$	Injected active/reactive power of *WF* installed in bus i into the grid at time t (pu)
$\cos\varphi_{lead}/\cos\varphi_{lag}$	Lead/lag power factor of *WF*s
λ	Loading parameter (pu)
$(P/Q)^{\max/\min}_i$	Maximum/minimum active/reactive power of substation i (pu)

$P_i^{WF,sd}$	Standard capacity of wind turbine installed at bus i (pu)
$I_{MAX_{ij}}$	Maximum current flow between buses i and j at *IOP* (pu)
$\hat{I}_{MAX_{ij}}$	Maximum current flow between buses i and j at *MLP* (pu)
$SOC_i^{\max/min}$	Maximum/minimum *SOC* of *ESS* installed at bus i (pu)
$N_{\max}^{WT}$	Maximum number of *WF*s that could be installed in the network
$N_{\max}^{ESS}$	Maximum number of *ESS*s that could be installed in the network
$\theta_{ij,t}$	Phase angle between buses i and j at time t at IOP
$\hat{\theta}_{ij,t}$	Phase angle between buses i and j at time t at MLP
$I_{R_{ij,t}}$	Real current flow component of branch between buses i and j at time t at *IOP* (pu)
$\hat{I}_{R_{ij,t}}$	Real current flow component of branch between buses i and j at time t at *MLP* (pu)
$K_{D,i}$	Rate of load change at bus i
$K_{G,i}$	Rate of change in active power of substation i
R_l	Resistance of line l (pu)
$SOC_{i,t}^{ESS}$	State of charge of *ESS* installed in bus i at time t (pu)
Δt	Timeslot duration (h)
$V_{i,t}$	Voltage magnitude of bus i at time t at *IOP* (pu)
$\hat{V}_{i,t}$	Voltage magnitude of bus i at time t at *MLP* (pu)
S_{base}	Base apparent power (*MVA*)
η_i^{WF}	An integer variable for number of wind turbines in *WF* i
$\eta_i^{WF,\max}$	Maximum number of wind turbines that could be installed in *WF* i

References

1. Fankhauser, S.; Smith, S.M.; Allen, M.; Axelsson, K.; Hale, T.; Hepburn, C.; Kendall, J.M.; Khosla, R.; Lezaun, J.; Mitchell-Larson, E.; et al. The meaning of net zero and how to get it right. *Nat. Clim. Chang.* **2021**, *12*, 15–21. [CrossRef]
2. Alahyari, A.; Pozo, D. Performance-based virtual power plant offering strategy incorporating hybrid uncertainty modeling and risk viewpoint. *Electr. Power Syst. Res.* **2021**, *203*, 107632. [CrossRef]
3. Alahyari, A.; Pozo, D. Online Demand Response for End-User Loads. In Proceedings of the 2019 IEEE Milan PowerTech, Milan, Italy, 23–27 June 2019; pp. 1–6. [CrossRef]
4. Nikkhah, S.; Sarantakos, I.; Zografou-Barredo, N.M.; Rabiee, A.; Allahham, A.; Giaouris, D. A Joint Risk-and Securi-ty-Constrained Control Framework for Real-Time Energy Scheduling of Islanded Microgrids. *IEEE Trans. Smart Grid* **2022**, *13*, 3354–3368. [CrossRef]
5. Alahyari, A.; Ehsan, M.; Moghimi, M. Managing distributed energy resources (DERs) through virtual power plant tech-nology (VPP): A stochastic information-gap decision theory (IGDT) approach. *Iran. J. Sci. Technol. Trans. Electr. Eng.* **2020**, *44*, 279–291. [CrossRef]
6. Global Wind Report 2022. Available online: https://gwec.net/global-wind-report-2022/ (accessed on 18 February 2023).
7. Farrokhifar, M.; Aghdam, F.H.; Alahyari, A.; Monavari, A.; Safari, A. Optimal energy management and sizing of renew-able energy and battery systems in residential sectors via a stochastic MILP model. *Electr. Power Syst. Res.* **2020**, *187*, 106483. [CrossRef]
8. Mousavizadeh, S.; Alahyari, A.; Bolandi, T.G.; Haghifam, M.; Siano, P. A novel resource allocation model based on the modularity concept for resiliency enhancement in electric distribution networks. *Int. J. Energy Res.* **2021**, *9*, 13471–13488. [CrossRef]
9. Rao, R.S.; Ravindra, K.; Satish, K.; Narasimham, S. Power loss minimization in distribution system using network reconfiguration in the presence of distributed generation. *IEEE Trans. Power Syst.* **2013**, *28*, 317–325. [CrossRef]
10. Franco, J.F.; Rider, M.J.; Lavorato, M.; Romero, R. A mixed-integer LP model for the reconfiguration of radial electric distribution systems considering distributed generation. *Electr. Power Syst. Res.* **2013**, *97*, 51–60. [CrossRef]
11. Asrari, A.; Wu, T.; Lotfifard, S. The Impacts of Distributed Energy Sources on Distribution Network Reconfiguration. *IEEE Trans. Energy Convers.* **2016**, *31*, 606–613. [CrossRef]
12. Kavousi-Fard, A.; Akbari-Zadeh, M.-R. Reliability enhancement using optimal distribution feeder reconfiguration. *Neurocomputing* **2013**, *106*, 1–11. [CrossRef]
13. Amanulla, B.; Chakrabarti, S.; Singh, S.N. Reconfiguration of Power Distribution Systems Considering Reliability and Power Loss. *IEEE Trans. Power Deliv.* **2012**, *27*, 918–926. [CrossRef]
14. Kavousi-Fard, A.; Niknam, T. Optimal distribution feeder reconfiguration for reliability improvement considering uncertainty. *IEEE Trans. Power Deliv.* **2014**, *29*, 1344–1353. [CrossRef]
15. Mazza, A.; Chicco, G.; Russo, A. Optimal multi-objective distribution system reconfiguration with multi criteria decision making-based solution ranking and enhanced genetic operators. *Int. J. Electr. Power Energy Syst.* **2014**, *54*, 255–267. [CrossRef]
16. Jeon, Y.-J.; Kim, J.-C.; Kim, J.-O.; Shin, J.-R.; Lee, K. An efficient simulated annealing algorithm for network reconfiguration in large-scale distribution systems. *IEEE Trans. Power Deliv.* **2002**, *17*, 1070–1078. [CrossRef]

17. Alonso, F.R.; Oliveira, D.Q.; de Souza, A.C.Z. Artificial Immune Systems Optimization Approach for Multiobjective Distribution System Reconfiguration. *IEEE Trans. Power Syst.* **2015**, *30*, 840–847. [CrossRef]
18. Narimani, M.R.; Vahed, A.A.; Azizipanah-Abarghooee, R.; Javidsharifi, M. Enhanced gravitational search algorithm for multi-objective distribution feeder reconfiguration considering reliability, loss and operational cost. *IET Gener. Transm. Distrib.* **2014**, *8*, 55–69. [CrossRef]
19. Nick, M.; Cherkaoui, R.; Paolone, M. Optimal Planning of Distributed Energy Storage Systems in Active Distribution Networks Embedding Grid Reconfiguration. *IEEE Trans. Power Syst.* **2017**, *33*, 1577–1590. [CrossRef]
20. Bai, L.; Jiang, T.; Li, F.; Chen, H.; Li, X. Distributed energy storage planning in soft open point based active distribution networks incorporating network reconfiguration and DG reactive power capability. *Appl. Energy* **2018**, *210*, 1082–1091. [CrossRef]
21. Santos, S.F.; Fitiwi, D.Z.; Cruz, M.R.; Cabrita, C.M.; Catalão, J.P. Impacts of optimal energy storage deployment and network reconfiguration on renewable integration level in distribution systems. *Appl. Energy* **2017**, *185*, 44–55. [CrossRef]
22. Nikkhah, S.; Rabiee, A. Optimal wind power generation investment, considering voltage stability of power systems. *Renew. Energy* **2018**, *115*, 308–325. [CrossRef]
23. Savier, J.S.; Das, D. Impact of Network Reconfiguration on Loss Allocation of Radial Distribution Systems. *IEEE Trans. Power Deliv.* **2007**, *22*, 2473–2480. [CrossRef]
24. Shuaib, Y.M.; Kalavathi, M.S.; Rajan, C.C.A. Optimal Reconfiguration in Radial Distribution System Using Gravitational Search Algorithm. *Electr. Power Compon. Syst.* **2014**, *42*, 703–715. [CrossRef]
25. Mohseni-Bonab, S.M.; Rabiee, A.; Mohammadi-Ivatloo, B. Voltage stability constrained multi-objective optimal reactive power dispatch under load and wind power uncertainties: A stochastic approach. *Renew. Energy* **2016**, *85*, 598–609. [CrossRef]
26. Nikkhah, S.; Rabiee, A.; Soroudi, A.; Allahham, A.; Taylor, P.C.; Giaouris, D. Distributed flexibility to maintain security margin through decentralised TSO–DSO coordination. *Int. J. Electr. Power Energy Syst.* **2023**, *146*, 108735. [CrossRef]
27. Mousavizadeh, S.; Alahyari, A.; Ghodsinya, S.R.M.; Haghifam, M.-R. Incorporating microgrids coupling with utilization of flexible switching to enhance self-healing ability of electric distribution systems. *Prot. Control Mod. Power Syst.* **2021**, *6*, 24. [CrossRef]
28. Ameli, A.; Bahrami, S.; Khazaeli, F.; Haghifam, M.-R. A multiobjective particle swarm optimization for sizing and placement of DGs from DG owner's and distribution company's viewpoints. *IEEE Trans. Power Deliv.* **2014**, *29*, 1831–1840. [CrossRef]
29. Baran, M.E.; Wu, F.F. Network reconfiguration in distribution systems for loss reduction and load balancing. *IEEE Trans. Power Deliv.* **1989**, *4*, 1401–1407. [CrossRef]
30. Brooke, A.; Kendrick, D.; Meeraus, A.; Raman, R.; Rosenthal, R. *GAMS: The Solver Manuals*; GAMS Development Corporation: Washington, DC, USA, 1998.
31. Nikkhah, S.; Rabiee, A. A Joint Energy Storage Systems and Wind Farms Long-Term Planning Model Considering Voltage Stability. In *Operation, Planning, and Analysis of Energy Storage Systems in Smart Energy Hubs*; Mohammadi-Ivatloo, B., Jabari, F., Eds.; Springer: Berlin, Germany, 2018; pp. 337–363.
32. Nikkhah, S.; Nasr, M.-A.; Rabiee, A. A Stochastic Voltage Stability Constrained EMS for Isolated Microgrids in the Presence of PEVs Using a Coordinated UC-OPF Framework. *IEEE Trans. Ind. Electron.* **2020**, *68*, 4046–4055. [CrossRef]